

THERMAL OPTIMIZATION AND VALDATION OF GaN HIGH
ELECTRON MOBILITY TRANSISTOR

BY

TANMAY PRADIP KAVADE

THESIS

Submitted in partial fulfilment of the requirements
for the degree of Master of Science in Mechanical Engineering at

The University of Texas at Arlington

May 2017

Arlington, Texas

Supervising Committee:

Dr Dereje Agonafer, Supervising Professor

Dr Abdolhossein Haji-Sheikh

Dr Andrey Beyle

Abstract

THERMAL OPTIMIZATION AND VALIDATION OF GaN HIGH ELECTRON MOBILITY TRANSISTOR

Tanmay Pradip Kavade

The University of Texas at Arlington, 2017

Supervising Professor: Dereje Agonafer

Gallium Nitride (GaN) is a binary III/V wide band gap semiconductor used in power electronics for operations at high power densities and high speeds. GaN has excellent characteristics like high break-down voltage, high thermal conductivity, and high electron saturation velocity which have led to an intensive study and wide use of GaN in many fields. Some of these fields range from amplifiers, MMIC, laser diodes, pulsed radars and counter-IED jammers to CAT-V modules and fourth generation infrastructure base-stations.

In this study package level thermal analysis and management of GaN high electron mobility transistor was carried out for determination of junction temperature and junction-case thermal resistance (R_{jc}). Two commercially

available models were used as a reference for analysis. The sizes for both the models were 3 × 3 mm and 4 × 4 mm with host substrate SiC and Si respectively. The model considers the thickness of GaN and host substrate layers, the gate pitch, length, width, and thermal conductivity of GaN, and host substrate. The analysis is carried out on FEA software.

Initially mesh sensitivity analysis was carried out to determine the best possible grid count for CFD analysis. Both the models were analyzed for steady state condition at various radio frequency power output to map the increment in the junction temperature. A parametric study is being carried out to optimize and reduce the maximum junction temperature and junction to case thermal resistance (R_{jc}) by providing convective air cooling and heat sink. The other part of this study includes optimization of the model using diamond as the host substrate and ceramic as mold compound material to monitor the decrease in the thermal resistance value. Comparative results in this study show the percentage reduction in the estimated R_{jc} value. Thermal resistance value is estimated using the below formula,

$$R_{jc} = \frac{T_j - T_c}{P}$$

From the results obtained a significant reduction in the estimated R_{jc} value was observed when compared for no flow, air flow with heat-sink, different host substrate and different mold compound material conditions. In

conclusion GaN HEMT can be optimized to achieve a significant improvement in operation. This would allow operation of GaN devices at high temperature without damaging the reliability and operation life-span.

Copyright © by Tanmay Pradip Kavade 2017

All Rights Reserved



Acknowledgement

I would like to thank my supervising professor Dr Agonafer for his constant support, and guidance on my thesis work. I would like to thank Mr. Alok Lohia – Texas Instruments for being my mentor and constantly guiding me and encouraging me throughout my work. I would also like to thank Dr. Abdolhossein Haji-Sheikh, Dr. Andrey Beyle for serving as committee members on my thesis.

I would also like to thank Ms. Sally Thompson, Ms. Debi Barton, and Ms. Flora Pinegar for assisting me through documentation and educational matters. My special thanks to our academic advisor Dr Nomura for his help. I would also like to thank the entire EMNSPC team.

I would also like to thank my family for helping me in my thesis with their presence emotionally and financially. Lastly this acknowledgement would not be complete without a special mention to my friends who have constantly supported me throughout my thesis.

May 1st, 2017

Table of Contents

Abstract	ii
Acknowledgement	vi
Table of Contents	vii
List of Illustrations.....	ix
List of Tables	xi
List of Nomenclature.....	xii
Chapter 1	13
Introduction.....	13
Chapter 2.....	15
Thesis Objective	15
Chapter 3.....	17
Manufacturing.....	17
Chapter 4.....	19
Methodology	19
4.1 Geometric Modelling.....	21
4.2 Mathematical Assumption.....	25
4.3 Material Properties.....	26
4.4 Printed Circuit Board.....	28
Chapter 5.....	30

Optimization and Validation.....	30
5.1 Boundary Condition.....	30
5.2 Validation.....	31
5.3 Forced convection heat transfer using air flow along with heat sink...32	
5.4 Comparative Study.....	32
Chapter.....	33
Results.....	33
6.1 Mesh Sensitivity.....	33
6.2 Validation.....	35
6.3 Forced convection heat transfer using air flow along with heat sink...37	
6.4 Comparative Study.....	39
Chapter 7.....	48
Conclusion.....	48
References	50
Biographical Information.....	57

List of Illustrations

Figure 1: Wurtzite Crystal Structure.....	13
Figure 2: Comparison of semiconductor material properties at room temperature	13
Figure 3: Modelling Simplifications	19
Figure 4: Modelling Assumption	20
Figure 5: Table containing Dimensions of variables	23
Figure 6: Thermal Vias in PCB	29
Figure 7: Graph of Mesh Sensitivity Analysis	34
Figure 8: Graph for R_{jc} VS RF Power Output.....	36
Figure 9: Maximum Junction Temperature values for various flow rates (Model 1)	38
Figure 10: Maximum Junction Temperature values for various flow rates (Model 2)	39
Figure 11: Graph for Maximum Junction Temperature VS RF Power Output.....	41
Figure 12: Junction-to-Case Thermal Resistance values for various cases (Model 1)	43
Figure 13: Junction-to-Case Thermal Resistance values for various cases (Model 2)	44

Figure 14: Junction-to-Case Thermal Resistance values for various cases (Model 2)	46
Figure 15: Junction-to-Case Thermal Resistance values for various cases (Model 2)	47

List of Tables

Table 1: Geometric Correlation of Model and actual package - Model 1 .	22
Table 2: Geometric Correlation of Model and actual package - Model 2 .	24
Table 3: Component Dimensions	25
Table 4: Tabulated RF Power Output	26
Table 5: Solid Material Properties.....	27
Table 6: Surface Properties	28
Table 7: Thermodynamic Properties of the PCB	29
Table 8: Boundary Conditions	31
Table 9: Mesh Sensitivity Analysis Data.....	34
Table 10: Junction-to-Case Thermal Resistance values for various RF Power Output.....	36
Table 11: Maximum Junction Temperature values for various flow rates	38
Table 12: Maximum Junction Temperature values for various RF Power Output.....	41
Table 13: Junction-to-Case Thermal Resistance values for various RF Power Output.....	43
Table 14: Junction-to-Case Thermal Resistance values for various RF Power Output.....	46

List of Nomenclature

GaN	Gallium Nitride
SiC	Silicon Carbide
Si	Silicon
ZnS	Zinc Sulphide
CFOM	Combined figure of merit
GaAs	Gallium Arsenide
Al	Aluminum
R_{jc}	Junction to case thermal resistance ($^{\circ}\text{C}/\text{W}$)
T_j	Junction Temperature ($^{\circ}\text{C}$)
T_c	Case temperature ($^{\circ}\text{C}$)
P	Power (W)
CFD	Computational Fluid Dynamics
HEMT	High Electron Mobility Transistor
FEA	Finite Element Analysis
MMIC	Monolithic Microwave Integrate Circuit.
IED	Improved Explosive Device
CAT	Community Antenna Television
RF	Radio-frequency

Chapter 1

Introduction

GaN is formed in Wurtzite structure, named after the mineral Wurtzite. This is an example of hexagonal crystal structure. The chemical prototype for this crystal structure is ZnS therefore it is also called as zinc blende crystal structure.

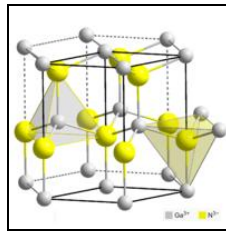


Figure 1: Wurtzite Crystal Structure

Below table shows the advantages of GaN

Property	Si	GaAs	4H-SiC	GaN
Bandgap $\cdot E_g$ (eV)	1.12	1.42	3.25	3.4
Dielectric constant $\cdot \epsilon$	11.8	12.8	9.7	9
Breakdown field E_c (MV/cm)	0.3	0.4	3	4
Electron mobility μ (cm ² /V-s)	1500	8500	1000	1250
Maximum velocity V_s (10 ⁷ cm/s)	1	1	2	3
Thermal conductivity λ (W/cm-K)	1.5	0.5	4.9	2.3
CFOM = $\lambda \epsilon \mu V_s E_c^2 / (\lambda \epsilon \mu V_s E_c^2)$ si	1	3.6	358	520

High-speed
High-power
High-temperature

- Si : lowest cost, large volume, bad Trr characteristic at HT.
- SiC : so far high crystal quality, but high cost.
- GaN : low cost, highest CFOM value.

Figure 2: Comparison of semiconductor material properties at room temperature

The increase in the demand for high power densities and high frequency has led to the application of GaN in many fields. From the above Figure 2: Comparison of semiconductor material properties at room temperature, it is evident that GaN performs the best in high speed, high power and high temperature application. GaN offers radio frequency power densities of high magnitude. On comparison GaN devices offer 2-3 times the power densities when compared with GaAs devices as seen in the table above.

Thermal management plays a pivotal role to utilize full potential of GaN devices. In finite element thermal simulation, the active device is replaced by a uniform heat source and the modelling effort is focused on the heat flow patterns. This approach allows for a more realistic evaluation along with the application of heat sink on top of the chip. In this study improvisation of heat dissipation has been carefully assessed to measure the effect of optimization on the entire system.

Chapter 2

Thesis Objective

The main objective and the motivation behind this study were also some of the issues that GaN devices suffer. These issues are as discussed below

1. Self-Heating

GaN devices suffer from excess heat generation. Even GaN on SiC which has excellent thermal conductivity together suffer from this issue. GaN on SiC devices have been observed to generate heat that causes the temperature to rise above 180°C.

2. Non-Uniform Distribution of Dissipated Power:

This issue results in hotspots within the GaN devices that degrade the drain current, output and gain of the system. It is also responsible for current dispersion and increase in the leakage current that further reduces the efficiency of the system

3. Mean Time to Failure:

The mean time to failure also abbreviated as MTTF reduces with increase in the temperature.

4. Thermal Resistance and Environmental Condition

Since GaN devices are high speed power and high temperature devices they need to be operated at correct thermal resistance values and proper environmental conditions.

5. Power Deration

When lateral GaN devices are operated at high power densities a considerable amount of electric field is generated which causes power deration to equipment's that are installed besides them.

Chapter 3

Manufacturing

The manufacturing process begins with the first passivation process which is done using SiN_x / SiO_2 . This is followed by a mesa isolation process also known as reactive ion etching. The chemical compound used in this process is HCl . This is followed by an evaporation of Au (Gold) and rapid thermal annealing (RTA) at 850°C for 30s in N_2 ambient to produce source and drain ohmic contacts. The 0.5 μm gate ohmic contacts are realized using photo resistor pattern where mask aligner is used to reduce manufacturing cost. The photo resistor patterning using mask aligner may sometime be replaced by electron beam lithography specifically when the 0.5 μm gate is fabricated in a T section in the source and the drain region. This is followed by a second round of rapid thermal annealing at same temperature (850°C for 30s) and ambience (N_2) and 2nd passivation process. The second passivation process is typically done to protect the device from oxidation and corrosion. After all these processes the GaN layer is developed on top of the desired substrate using MOCVD (Metal organic chemical vapor deposition).

In metal, organic chemical vapor deposition (MOCVD) the metal organic compounds like Ga, Al, In are supplied using compounds like

trimethylgallium, trimethylaluminium, trimethylindium. These compounds are carried by carrier gas which is usually hydrogen. The concentration of the compound in the carrier gas is determined with the help of vapor pressure. In a standard MOCVD process a thin nucleation layer of AlN of 20 – 200nm is grown using ammonia and trimethylaluminium. GaN layer nucleates on this AlN up to a thickness of 1 to 2 μm . The initial layer of the GaN is not good however the quality improves as the growth proceeds. Usually the host substrate material on which the AlN layer is developed is SiC due to its high thermal conductivity; however Si and sapphire are also used for low cost. The ternary alloy barrier layer such as AlGaN is grown using compounds like trimethylaluminium and trimethylgallium. The difference in the electronic band between GaN and AlGaN is responsible for the presence of the high concentration 2DEG (Dimensional Electron Gas) layer.

This 2DEG channel is responsible for releasing the charge when negative voltage is applied across the gate (Negative bias) whereas it allows the charge into the channel when positive voltage (Positive bias) or zero voltage is applied. In the On-state the current flows through the device whereas in the OFF-state the current flow has to be restricted in an ideal case. However that is never possible due to certain non-idealities and leakage.

Chapter 4

Methodology

Numerical simulation offers a complementary path for thermal evaluation. However electro-thermal modelling is a formidable task since it requires accurate physical modelling of the entire structure that needs to account for the pyroelectric, piezoelectric and polar nature of the materials. This leads to wastage of time and energy which requires a lot of parameter tweaking. In meshing the entire structure, a very fine mesh is required for the active device which reduces the grid size to nanometers. Therefore certain modifications and simplifications are necessary to reduce efforts and computational time.

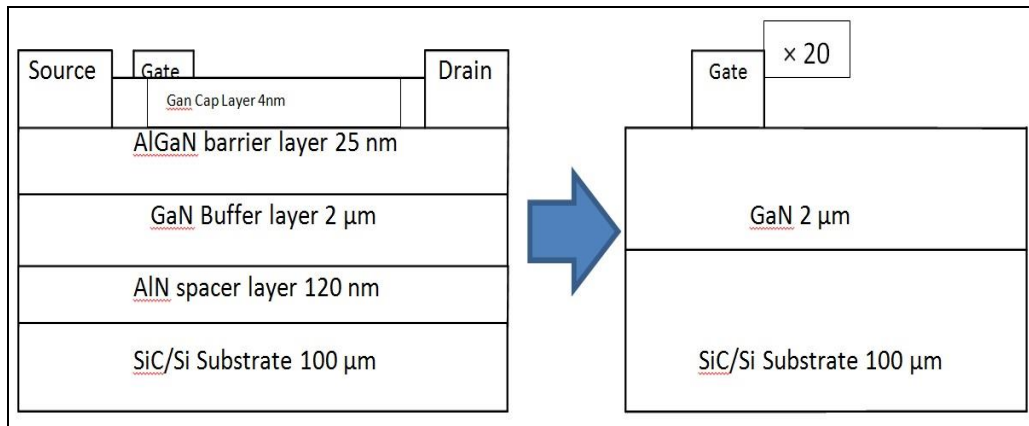


Figure 3: Modelling Simplifications

As seen in the Figure 3: Modelling Simplifications above the structure of GaN HEMT is shown on the left and its simplification is shown on the right. The GaN HEMT has certain layers that have thickness in nanometer scale. Since this layers are extremely small in dimension their contribution towards the heat transfer is negligible and therefore it is advisable to neglect these layers to reduce the load on computation and save resources. In a GaN HEMT the gate is the only heat generating source and therefore it is safe to neglect the source and the drain during modelling for finite element analysis.

Finite Element analysis (FEA) is conducted using ansys icepak to determine the temperature distribution and the maximum junction temperature. As an example a standard layout of multi-finger GaN HEMT for RF application is as shown in the figure below.

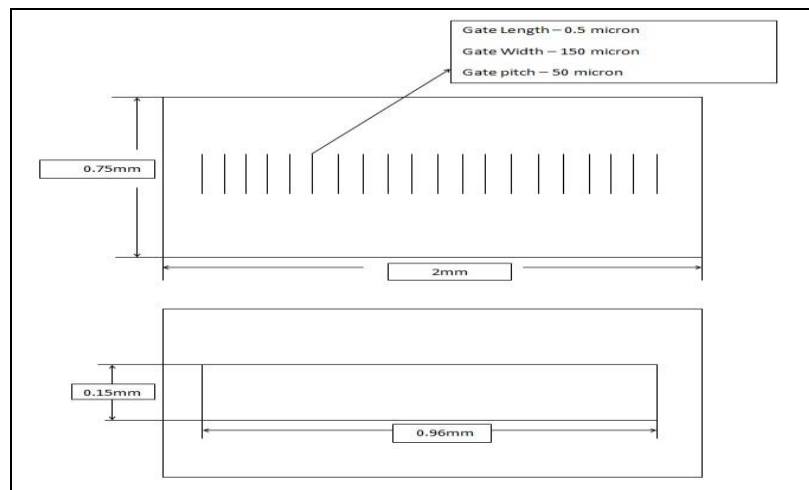


Figure 4: Modelling Assumption

As shown in the Figure 4: Modelling Assumption above, all the gates have a length ($L_g = 0.5 \mu\text{m}$), width ($W_g = 150 \mu\text{m}$) and gate pitch ($L_p = 50 \mu\text{m}$).

The study carried out is purely thermal simulation on finite element software. Therefore the active device is replaced by a uniform heat source placed on top of the GaN layer as seen in fig b. The modelling effort in this study is completely focused on simulation of heat flow. This approach allows for a much more realistic evaluation of static self-heating.

4.1 Geometric Modelling

The two models referenced in this study were prepared using two commercially available models. The external dimensions used in the modelling are exactly the same as shown in the data sheet. However the internal dimensions were assumed for the purposes of theoretical study. Dimensions of components like exposed pad, mold compound, lead pin are the same as mentioned in the data sheet.

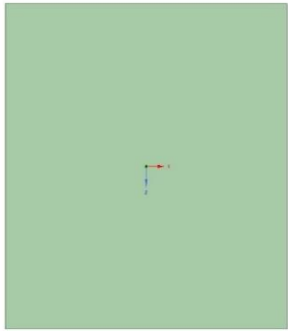
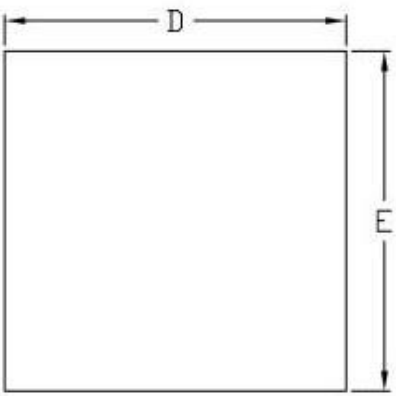
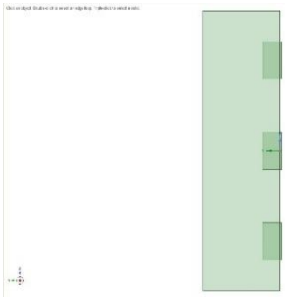
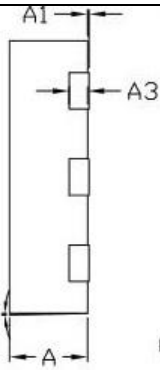
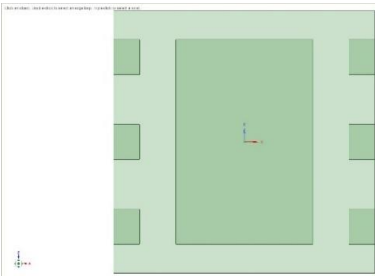
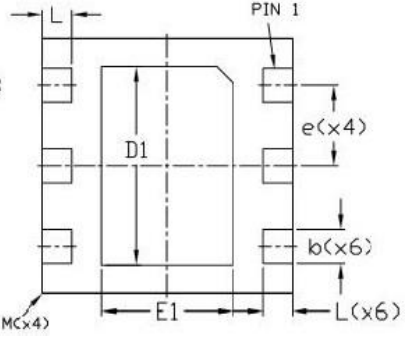
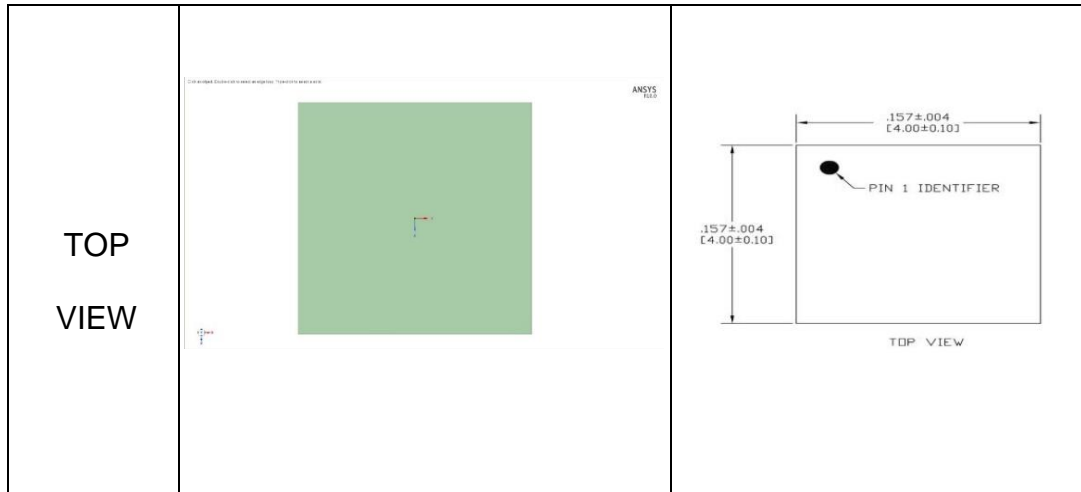
<p>TOP VIEW</p>		
<p>SIDE VIEW</p>		
<p>BOTTOM VIEW</p>		

Table 1: Geometric Correlation of Model and actual package - Model 1

DIM	MILLIMETERS			INCHES		
	MIN	NOM	MAX	MIN	NOM	MAX
A	0.80	0.90	1.00	0.032	0.035	0.039
A1	0	0.02	0.05	0	0.0008	0.002
A3	—	0.20REF.	—	—	0.008REF.	—
b	0.30	0.40	0.45	0.012	0.016	0.018
D	2.85	3.00	3.15	0.112	0.118	0.124
D1	—	2.34BSC	—	—	0.092BSC	—
E	2.85	3.00	3.15	0.112	0.118	0.124
E1	—	1.57BSC	—	—	0.062BSC	—
e	—	0.95BSC	—	—	0.037BSC	—
L	0.20	0.30	0.45	0.008	0.012	0.018
θ	0	—	12	0	—	12
M	—	—	0.05	—	—	0.002

Figure 5: Table containing Dimensions of variables



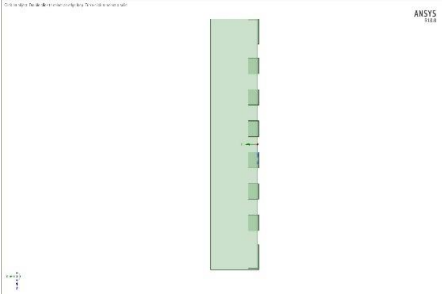
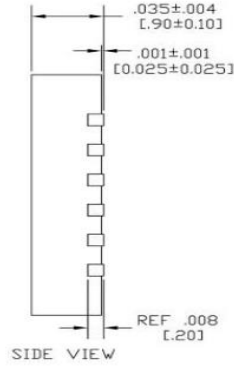
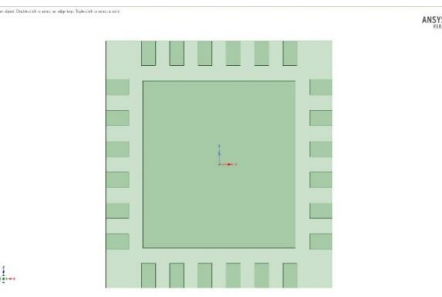
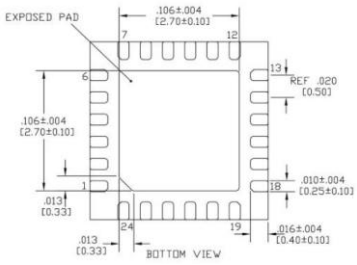
<p style="text-align: center;">SIDE VIEW</p>		 <p style="text-align: center;">SIDE VIEW</p>
<p style="text-align: center;">BOTTOM VIEW</p>		 <p style="text-align: center;">BOTTOM VIEW</p>

Table 2: Geometric Correlation of Model and actual package - Model 2

Assumed Dimensions are as shown in the table below: -

COMPONENT	DIMENSION	UNITS
Heat Source	0.15 × 0.96 × 0.005	MM
Die (GaN Layer)	0.75 × 2 × 0.002	MM
Die (SiC Layer)	0.75 × 2 × 0.1	MM
Die Attach	0.75 × 2 × 0.2	MM

Table 3: Component Dimensions

Same dimensions for the components mentioned above are used for model 2. The only difference between Model 1 and Model 2 is the overall footprint, and dimension of the exposed pad.

4.2 Mathematical Assumption

For the simplicity of heat transfer simulation, the power values used are not RF power output instead an assumption is made wherein the DC power input is completely dissipated as heat. This DC power input is used for the evaluation of RF power output using the formula mentioned below,

$$P_{\text{diss}} = (P_{\text{rf(output)}} - P_{\text{rf(input)}}) \times \left[\frac{1}{\text{P.A.E}} - 1 \right]$$

In the above formula a gain of 10% and a P.A.E (Power added efficiency) of 40% is being considered. This is the least value a HEMT can have.

Gain can also be represented as below

$$\frac{P_{rf(output)}}{P_{rf(input)}} = 1$$

Based on the above formula Radio-frequency power output is tabulated in excel as shown below-

Sr No	P _{diss} (W)	P _{rf(output)} (W)
1	1	0.74
2	1.5	1.11
3	2	1.48
4	2.5	1.85
5	3	2.22
6	3.5	2.6
7	4	2.96
8	4.5	3.7

Table 4: Tabulated RF Power Output

4.3 Material Properties

To get an actual representation of the model it is important to use accurate material properties. Ansys icepak has the option to manually set solid material as well as surface properties which are desired. Below table shows the material properties

4.3.1 Solid Material Properties

OBJECT	MATERIAL	PROPERTIES
GaN Layer	GaN	Density – 6.15 g/cm ³ Specific Heat - 487.28 J/Kg-K Conductivity – 150 W/m-K
Lead Anchor / Lead Pin	SAC 305	Density – 7.38 g/cm ³ Specific Heat - 0.05497J/Kg-K Conductivity – 63.2 W/m-K
Die Attach Material	AuSn	Density – 14700 Kg/m ³ Specific Heat – 150 J/Kg-C Conductivity – 57 W/m-K

Table 5: Solid Material Properties

4.3.2 Surface Properties

OBJECT	MATERIAL	PROPERTIES
Lead Pin/Exposed pad	Sn Platte	Roughness – 0.0 m Emissivity – 0.04 Solar behavior – Opaque Solar Absorptance - normal incidence – 0.186 Hemispherical diffuse absorptance – 0.186

Table 6: Surface Properties

4.4 Printed Circuit Board

All chips whether they are HEMT, Power amplifiers, Monolithic microwave integrated circuit (MMIC) all are mounted on a PCB board. So in order to have a better understanding of the heat transfer mechanism it important to give proper consideration to the thermal characteristics of the PCB board.

The PCB board used in this study is referenced from a commercially available model. It has the following mentioned stack-up of copper layers

1st Layer - 250 μ m - 80% Coverage.

2nd, 3rd, 4th Layer - 150 μ m – 70% Coverage.

The thermal vias for proper heat dissipation is as shown in the Figure 6:

Thermal Vias in PCB below

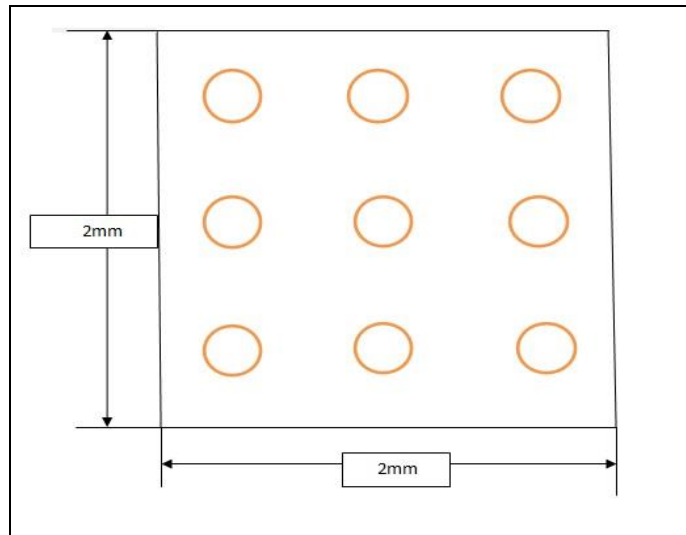


Figure 6: Thermal Vias in PCB

Each thermal vias is 0.4mm in dimensions. All the thermal vias are copper plated with FR4 filling in them.

The thermodynamic properties of the PCB are as seen in the table below

SR NO	DESCRIPTION	VALUE	UNITS
1	Density	1860	Kg/m ³
2	Specific Heat	960	J/Kg-K
3	Conductivity	0.69	W/m-K

Table 7: Thermodynamic Properties of the PCB

Chapter 5

Optimization and Validation

5.1 Boundary Condition

The below table shows the boundary condition used for various faces of the cabinet in ansys icepack.

SR NO	PLANE	TYPE	BOUNDARY CONDITION
1	X_{min}	Impermeable adiabatic boundary	$Q=0$
2	X_{max}	Impermeable adiabatic boundary	$Q=0$
3	Y_{min}	Wall	Constant Temperature - 25°C
4	Y_{max}	Impermeable adiabatic boundary	$Q=0$
5	Z_{min}	Opening	<ul style="list-style-type: none">• Flow – 1, 2, 3 m/sec only for convective heat transfer optimization.• No flow for validation and comparative study.

6	Z_{max}	Opening	<ul style="list-style-type: none"> • Flow – 1, 2, 3 m/sec only for convective heat transfer optimization. • No flow for validation and comparative study.
---	-----------	---------	---

Table 8: Boundary Conditions

The Y_{min} is maintained at 25°C since maximum amount of heat flows in the downward direction due to larger surface area. Therefore, to simulate the model for better heat transfer characteristics Y_{min} is maintained at a constant temperature i.e. isothermal boundary.

5.2 Validation

Both the models were validated with the commercially available models using junction to case thermal resistance values. This is important since validation gives a better understanding of the effects of optimization techniques which can be implemented in practical situation.

5.3 Forced convection heat transfer using air flow along with heat sink

GaN HEMT generate a lot of heat during operation at radio-frequency power output. Therefore, forced convection heat transfer serves as a good cooling technique to achieve reduction in the maximum junction temperature. Air flow velocities of 1, 2, 3 m/secs were studied to map the reduction in the thermal resistance values and the maximum junction temperature.

5.4 Comparative Study

In this study, maximum junction temperature, and Junction to case thermal resistance values (R_{jc}) were compared for various cases,

1. Maximum junction temperature for SiC and Si as substrate material
2. Junction to case thermal resistance values for no flow, flow with Heat sink and diamond as host substrate material
3. Junction to case thermal resistance values (R_{jc}) for ceramic and standard epoxy as mold compound material.

Chapter 6

Results

6.1 Mesh Sensitivity

To achieve good results, the grid or mesh applied to the model needs to be refined. The measure of refining the mesh is known as mesh sensitivity analysis. It ensures the results are mesh size and count independent. For our model, we varied the mesh count from 3.5 million to 15 million and found the maximum junction temperature be constant after the mesh count of 15 million. To save the computational time, we carried out analysis at 15 million mesh count.

Max Elements	Max Element size (mm)			Temperature	
	X	Y	Z	Model 2	Model 1
3520509	7	7	7.5	165.554	174.886
3668099	3	3	3.5	161.973	169.63
3839493	2.5	2.5	3	160.674	167.84
5117293	1	1	1.5	158.143	164.917
5393629	0.9	0.9	1.45	157.75	164.756
5494319	0.85	0.85	1.4	157.691	164.452
5713111	0.8	0.8	1.35	157.608	164.647

7939922	0.5	0.5	1	157.294	163.773
8571469	0.45	0.45	0.95	157.288	163.24
9579926	0.4	0.4	0.9	157.007	163.24
10680533	0.35	0.35	0.85	156.648	162.984
12452373	0.3	0.3	0.8	156.247	162.343
15093005	0.25	0.25	0.75	156.247	162.343

Table 9: Mesh Sensitivity Analysis Data

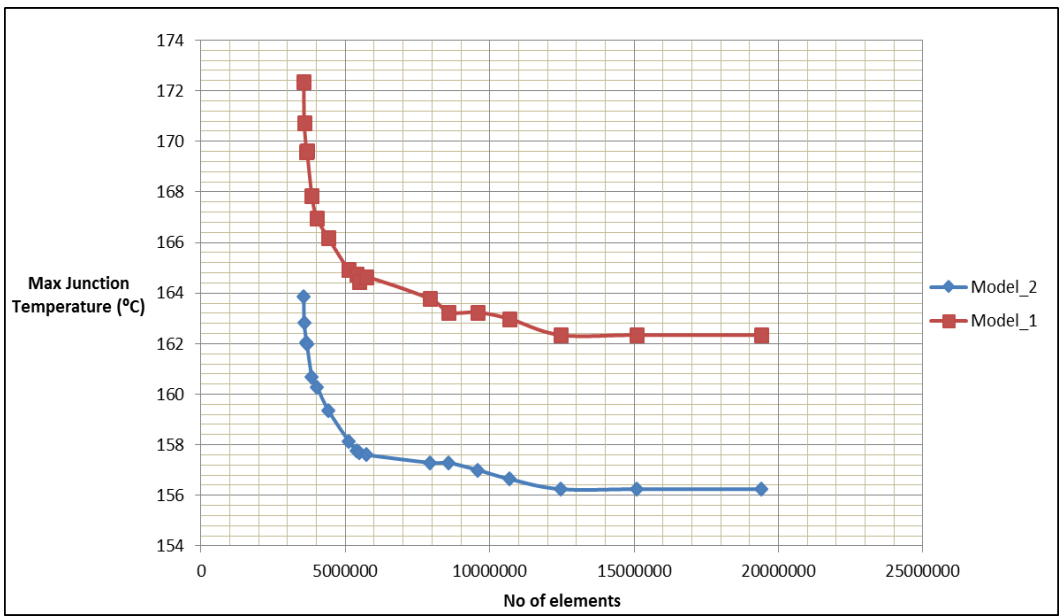


Figure 7: Graph of Mesh Sensitivity Analysis

6.2 Validation

As discussed in the section 5.2 both the models were validated using commercially available models by comparing the junction to case thermal resistance values. The commercial models have junction to case thermal resistance values of 10.5 °C/W and 12 °C/W. On simulating both the models in ansys icepak an average junction to case thermal resistance value of 11.5 and 12.1 was observed as shown in the table and Figure 8: Graph for Rjc VS RF Power Output.

Trail	Maximum Junction temp(°C)		Case temp(°C)		Power (W)	Rjc (°C/W)	
	Model 1	Model 2	Model 1	Model 2		Model 1	Model 2
Trail-1	64.95	67.51	56.38	58.62	0.74	11.581	12.010
Trail-2	85.09	89.21	72.23	75.87	1.11	11.585	12.017
Trail-3	105.2	110.7	88.09	92.87	1.48	11.560	12.042

Trail-4	125.4	132.2	103.9	109.96	1.85	11.621	12.022
Trail-5	145.5	153.7	119.8	127.01	2.22	11.576	12.020
Trail-6	166.2	175.8	136.1	144.57	2.6	11.576	12.009
Trail-7	185.8	196.8	151.5	161.25	2.96	11.587	12.007
Trial-8	226.1	240.1	183.2	195.62	3.7	11.594	12.02

Table 10: Junction-to-Case Thermal Resistance values for various RF

Power Output

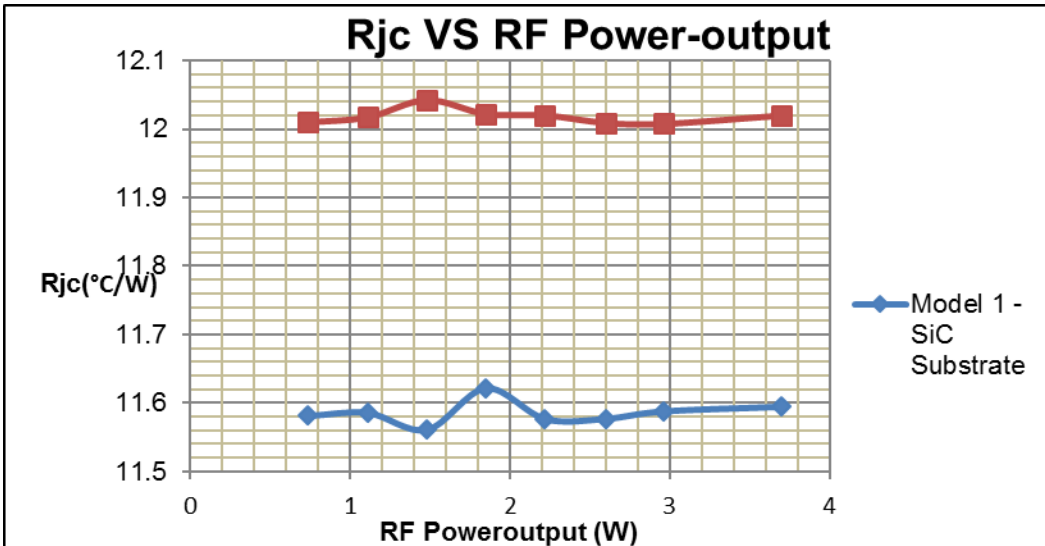


Figure 8: Graph for Rjc VS RF Power Output

A deviation of 8.7% and 0.8% is observed from the actual value which is in good agreement.

6.3 Forced convection heat transfer using air flow along with heat sink

As Discussed in section 5.3 air flow is provided along with heat sink mounted on top of the GaN HEMT. The results obtained from simulation are as shown in the table and Figure 9: Maximum Junction Temperature values for various flow rates (Model 1) and Figure 10: Maximum Junction Temperature values for various flow rates (Model 2) below,

Trail	Power (W)	Temperature (°C)					
		Model 1			Model 2		
		1(m/s)	2(m/s)	3(m/s)	1(m/s)	2(m/s)	3(m/s)
Trail-1	0.74	57.37	55.62	55.94	54.76	53.39	53.29
Trail-2	1.11	74.52	71.92	72.31	70.48	68.69	68.99
Trail-3	1.48	91.59	88.42	87.88	86.13	83.74	83.22

Trail-4	1.85	108.5	105	102.4	101.8	98.54	97.16
Trail-5	2.22	125.4	121.7	116.9	117.5	113.4	110.9
Trail-6	2.6	143.2	138.8	131.9	133.7	129.1	125.1
Trail-7	2.96	160.7	154.3	145.9	149.5	144	138.5
Trial-8	3.7	196.2	186.5	175.3	181.7	173.7	166

Table 11: Maximum Junction Temperature values for various flow rates

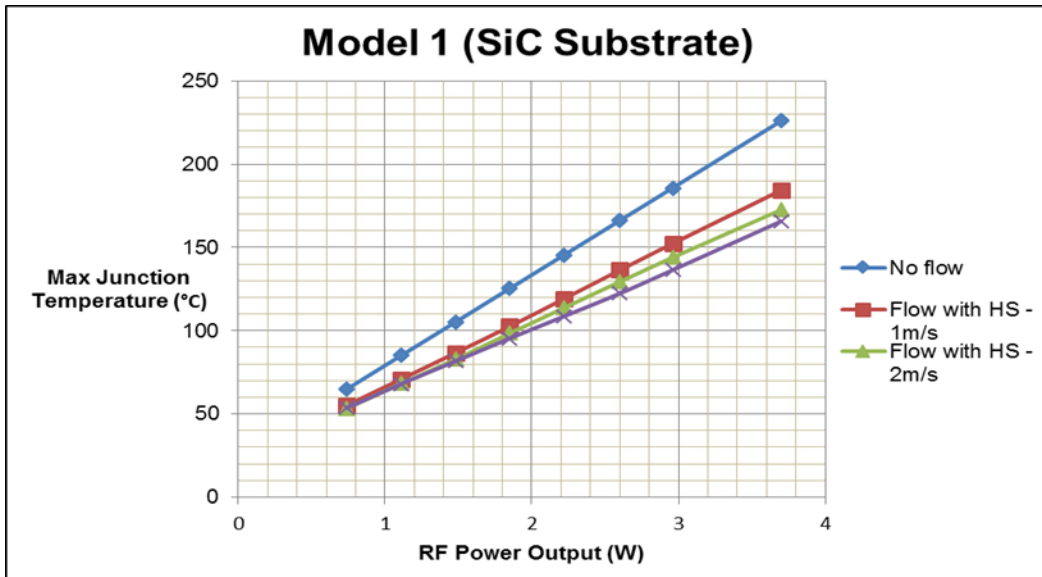


Figure 9: Maximum Junction Temperature values for various flow rates

(Model 1)

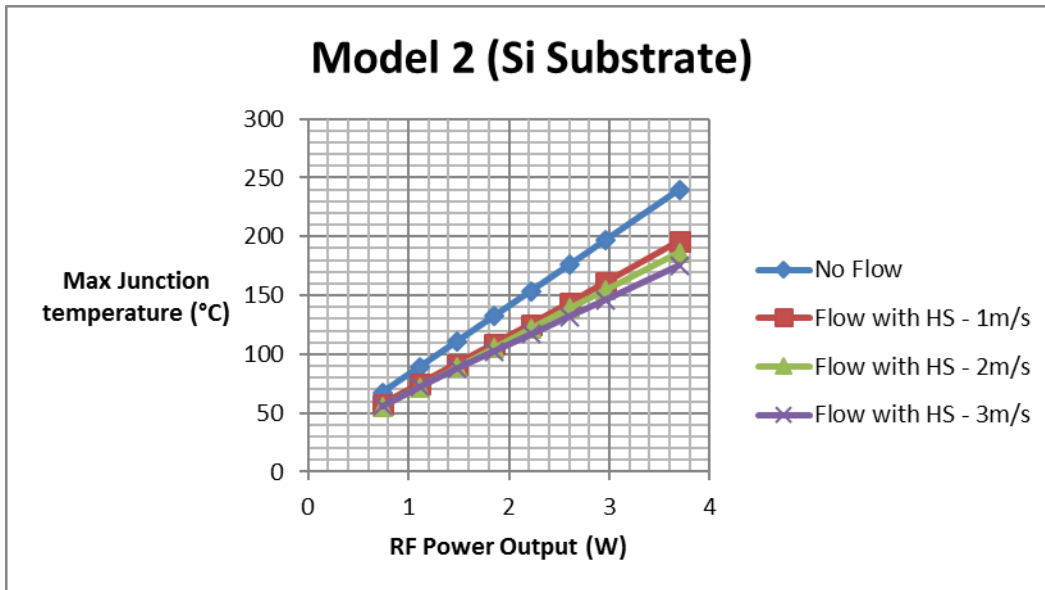


Figure 10: Maximum Junction Temperature values for various flow rates (Model 2)

Optimization techniques such as these can be applied to practical use in order to broaden the spectrum of operation for GaN HEMT.

6.4 Comparative Study

6.4.1 Maximum junction temperature for SiC and Si as substrate material.

Both the models were simulated for various RF power outputs for comparison of maximum junction temperature. The results of the

simulation are as shown in the table and Figure 11: Graph for Maximum Junction Temperature VS RF Power Output below

Trail	Maximum Junction Temp (°C)		Power (W)
	Model 1	Model 2	
Trail-1	64.95	67.51	0.74
Trail-2	85.09	89.21	1.11
Trail-3	105.2	110.7	1.48
Trail-4	125.4	132.2	1.85
Trail-5	145.5	153.7	2.22
Trail-6	166.2	175.8	2.6
Trail-7	185.8	196.8	2.96

Trail-8	226.1	240.1	3.7
---------	-------	-------	-----

Table 12: Maximum Junction Temperature values for various RF Power Output

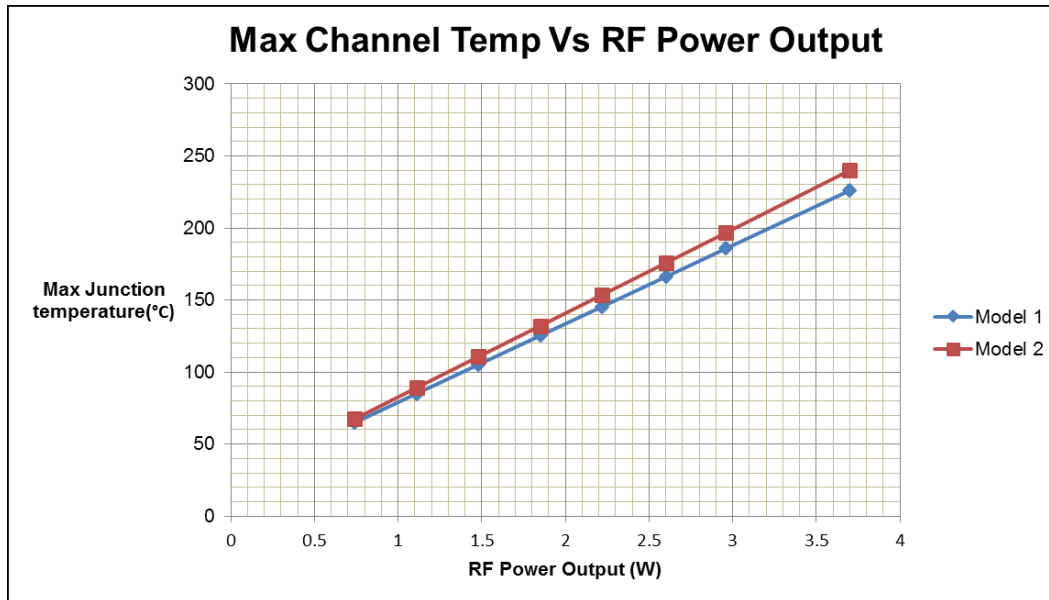


Figure 11: Graph for Maximum Junction Temperature VS RF Power Output

As observed from the Figure 11: Graph for Maximum Junction Temperature VS RF Power Output for Model 1 (SiC substrate) has a lower maximum junction temperature when compared to Model 2 (Si Substrate). This shows that SiC serves as an excellent host substrate material when downsizing a package for saving space.

6.4.2 Junction to case thermal resistance values for no flow, flow with Heat sink and diamond as host substrate material

A comparative study was conducted to note the reduction in the R_{jc} value. The simulation data is shown in the table below along with the Figure 12: Junction-to-Case Thermal Resistance values for various cases (Model 1) and Figure 13: Junction-to-Case Thermal Resistance values for various cases (Model 2)

Trail	Power (W)	$R_{jc} (^{\circ}C/W)$					
		No Flow		Flow with Heat-Sink		Diamond – Host Substrate	
		Model 1	Model 2	Model 1	Model 2	Model 1	Model 2
Trail-1	0.74	11.58	12.010	10.05	8.878	9.472	4.1081
Trail-2	1.11	11.58	12.017	10.24	8.891	9.468	4.1081
Trail-3	1.48	11.56	12.042	10.32	8.898	9.459	4.1283
Trail-4	1.85	11.62	12.022	10.37	8.913	9.459	4.1081
Trail-5	2.22	11.57	12.020	10.42	8.918	9.504	4.0990
Trail-6	2.6	11.576	12.009	10.457	8.923	9.461	4.1153
Trail-7	2.96	11.587	12.007	10.522	8.918	9.459	4.0878

Trial-8	3.7	11.594	12.02	10.585	8.9189	9.459	4.0810
---------	-----	--------	-------	--------	--------	-------	--------

Table 13: Junction-to-Case Thermal Resistance values for various RF

Power Output

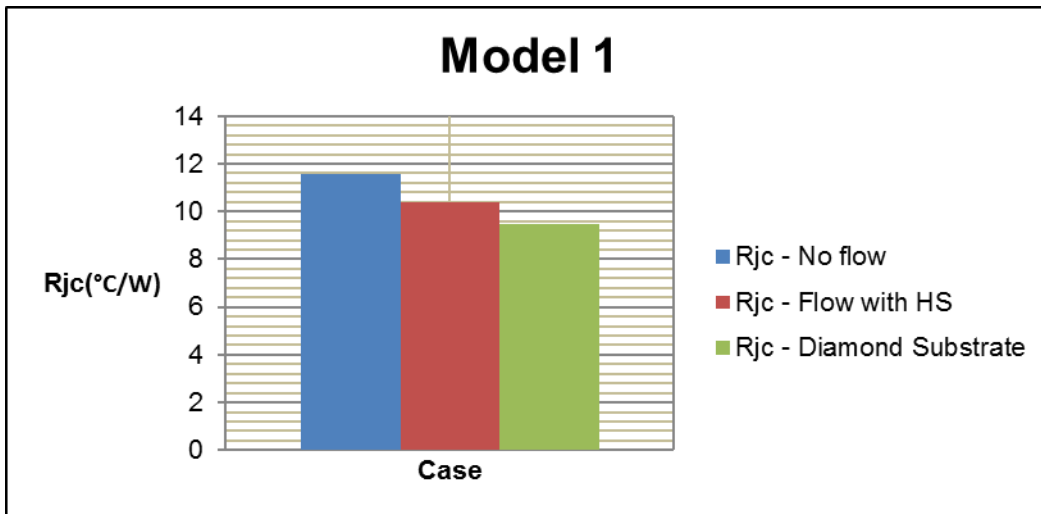


Figure 12: Junction-to-Case Thermal Resistance values for various cases

(Model 1)

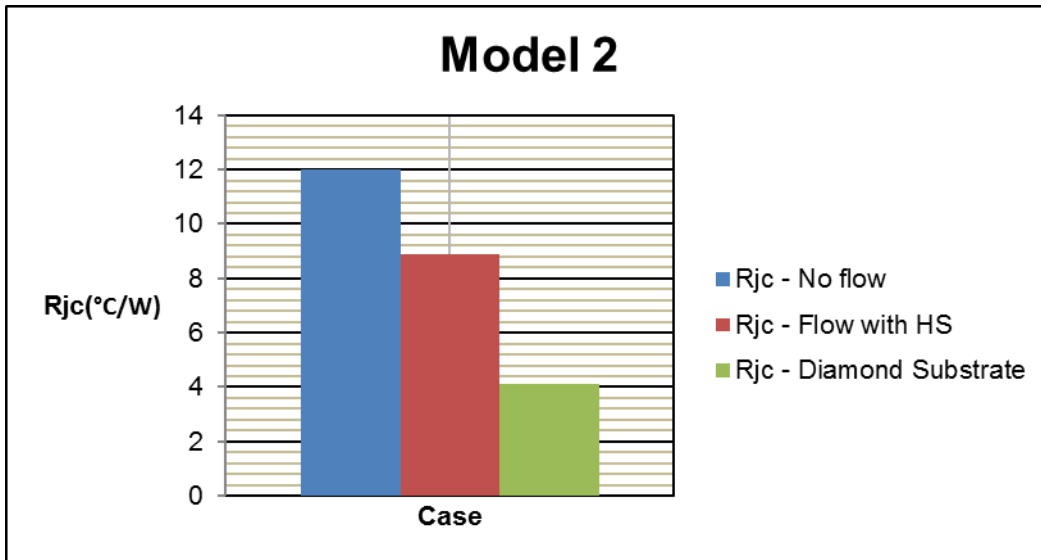


Figure 13: Junction-to-Case Thermal Resistance values for various cases
(Model 2)

From the above graph we observe that the thermal resistance reduces by 13% when air flow with Heat sink is used on top of the package and it reduces by 18% when diamond is used as the host substrate material. A similar trend is followed for Model 2 however the reduction is higher with 26% for air flow with heat sink and 66% when diamond is used as the host substrate material.

6.4.3 Junction to case thermal resistance values (R_{jc}) for ceramic and standard epoxy as mold compound material.

In this study thermal resistance (R_{jc}) values for ceramic and standard epoxy mold compound material were observed to measure the reduction. Ceramic has good thermal properties as compared to standard epoxy. It will interesting to see the variation across both the models when ceramic is used. Following table and Figure 14: Junction-to-Case Thermal Resistance values for various cases (Model 2) and Figure 15: Junction-to-Case Thermal Resistance values for various cases (Model 2) shows the data obtained from simulation,

Trail	Power(W)	$R_{jc} (^{\circ}\text{C/W})$			
		Model 1		Model 2	
		Standard Epoxy	Ceramic	Standard Epoxy	Ceramic
Trail-1	0.74	11.581	6.527027	12.0102	6.824324
Trail-2	1.11	11.585	6.522523	12.0173	6.828829
Trail-3	1.48	11.560	6.547297	12.0423	6.824324

Trail-4	1.85	11.621	6.486486	12.0221	6.810811
Trail-5	2.22	11.576	6.531532	12.0202	6.846847
Trail-6	2.6	11.576	6.538462	12.0092	6.846154
Trail-7	2.96	11.587	6.52027	12.0077	6.824324
Trial-8	3.7	11.594	6.540541	12.02	6.837838

Table 14: Junction-to-Case Thermal Resistance values for various RF Power Output

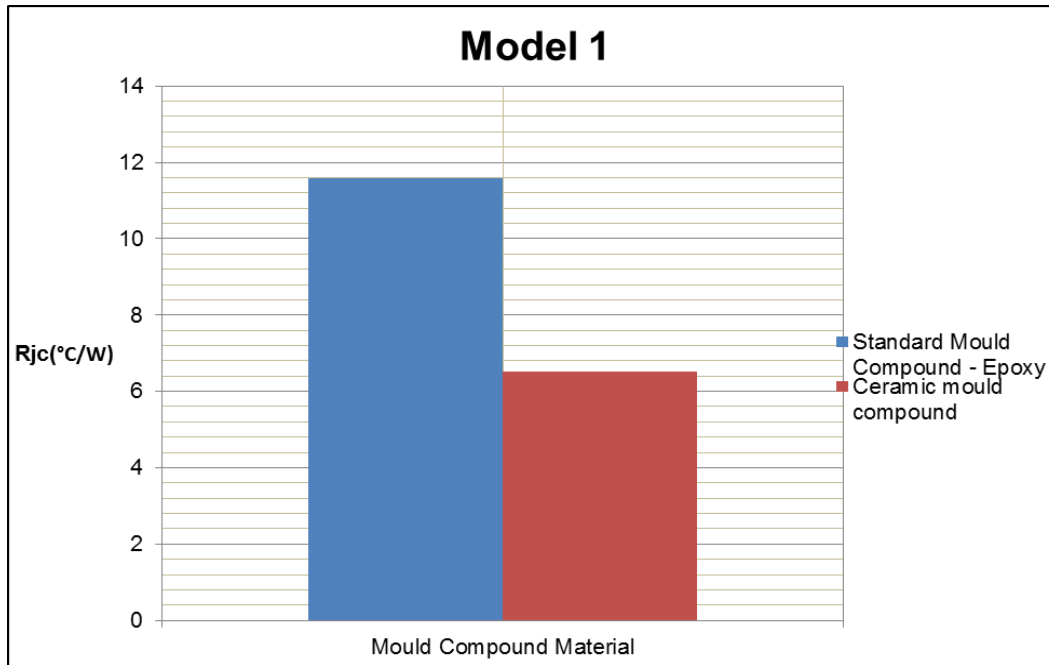


Figure 14: Junction-to-Case Thermal Resistance values for various cases (Model 2)

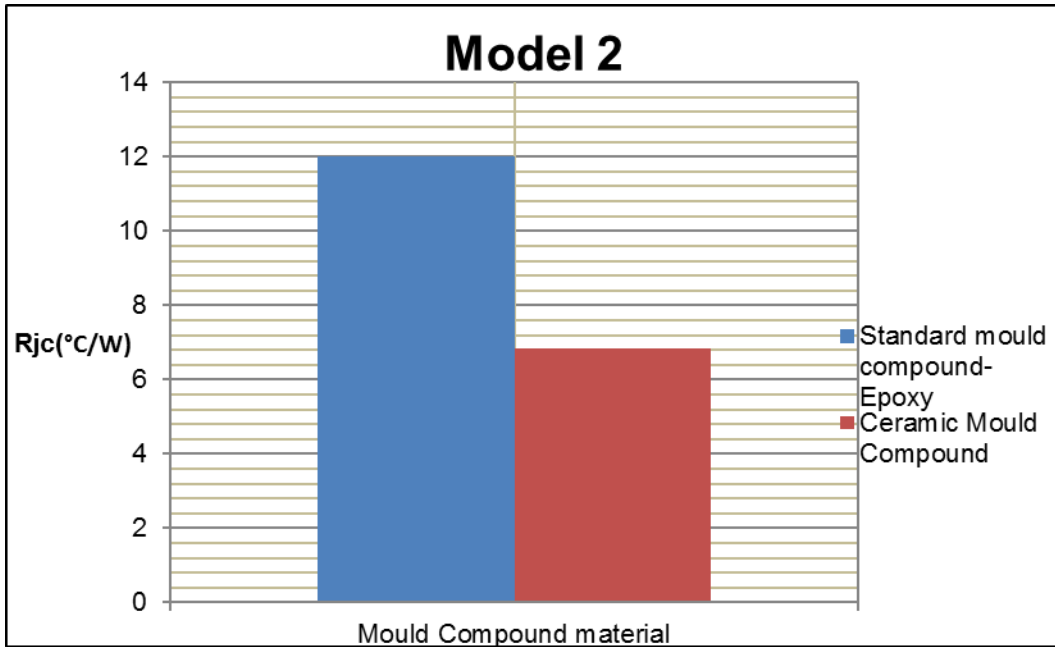


Figure 15: Junction-to-Case Thermal Resistance values for various cases
(Model 2)

When ceramic is used as a mold compounding material a reduction of 45% by average is observed for both the Models.

Chapter 7

Conclusion

In conclusion, detailed CFD model for 2 GaN HEMT was developed using commercially available models.

- Both the models are validated using junction to case thermal resistance values (R_{jc}). A deviation of 8.7 and 0.8% is observed in the R_{jc} value which is in good agreement. Hence we can say that both the models are validated.
- Both the models are simulated at various Radio-frequency power outputs. From the results, we observe that SiC servers as a better host substrate material when miniaturization of package is done for saving space.
- A reduction of 10% and 25% is observed in the thermal resistance values when optimization technique with convective heat transfer using air flow with heat sink is being used. This observation would enable designers to operate the GaN device at a higher radio-frequency power output without the risk of damaging the device and further increasing the envelope of operation.

- Diamond serves as an excellent host substrate material due to its higher thermal conductivity. Comparative results discussed in this study show a reduction of 18% and 66% in the thermal resistance values.
- In this study, ceramic has been used as the mold compound material instead of standard epoxy. It is observed that a reduction of 45% by average is being achieved in the thermal resistance values.

References

- Device-Level Thermal Analysis of GaN-based Electronics
Kevin Robert Bagnall, MIT, June 2013, Partial fulfilment of the Requirements for the Degree of Masters of Science in Mechanical Engineering.
- Three-dimensional finite-element thermal simulation of GaN-based HEMTs
F. Bertoluzza, N. Delmonte *, R. Menozzi
University of Parma, Dipartimento di Ingegneria dell'Informazione, Viale G.P. Usberti, 181/A, 43100 Parma, Italy
- Improvement of thermal management of high-power GaN-based Light-emitting diodes
Bo-Hung Liou^a, Chih-Ming Chen^{a,*}, Ray-Hua Horng^b, Yi-Chen Chiang^c, Dong-Sing Wu^d
a Department of Chemical Engineering, National Chung Hsing University, Taichung 402, Taiwan
b Department of Electro-Optical Engineering, National Cheng Kung University, Tainan 701, Taiwan

c Institute of Precision Engineering, National Chung Hsing University,
Taichung 402, Taiwan

d Department of Materials Science and Engineering, National Chung
Hsing University, Taichung 402, Taiwan

- Thermal optimization of GaN-on-Si HEMTs with plastic package

R. Liu^{a, b,*}, D. Schreurs^a, W. De Raedt^b, F. Vanaverbeke^b, R.
Mertens^{a,b}, I. De Wolf^{b,c},

a Department of Electrical Engineering, K.U. Leuven, Kasteelpark
Arenberg 10, 3001 Leuven, Belgium.

b Department of Metallurgy and Materials Engineering, K.U. Leuven,
Kasteelpark Arenberg 44, 3001 Leuven, Belgium

- Evaluation of GaN Transistors Having Two Different Gate-Lengths for
Class-S PA Design

Jun-Chul Park¹ · Chan-Sei Yoo² · Dongsu Kim³ · Woo-Sung Le² · Jong-
Gwan Yook^{1,*}.

1- Electrical and Electronic Engineering Department, Yonsei
University, Seoul, Korea.

2- Electronic Materials & Device Research Center, Korea Electronics
Technology Institute, Seongnam, Korea.

3- Packaging Research Center, Korea Electronics Technology Institute, Seongnam, Korea.

- High heat flux cooling solutions for thermal management of high power density gallium nitride HEMT

Avijit Bhunia, Karim Boutros, Chung-Lung Chen, Rockwell Scientific Company

1049 Camino Dos Rios, Thousand Oaks, CA91360, USA, Phone: (805) 3734348

Fax: (805) 3734860, Email: abhunia@nvsc.com

- A review of GaN on SiC high electron-mobility power transistors and MMICs

Article in IEEE Transactions on Microwave Theory and Techniques · June 2012

DOI: 10.1109/TMTT.2012.2187535

- Thermal Analysis and its application to high power GaN HEMT Power Amplifiers, A. Prejjs, S. Wood, R. Pengelly, W. Pribble, Cree Inc., Durham, NC 27703 USA.

- https://en.wikipedia.org/wiki/Gallium_nitride
- Thermal analysis of high power GaN-based LEDs with ceramic package
Lianqiao Yang, Sunho Jang, Woongjoon Hwang, Moowhan Shin
- Thermal and Mechanical Analysis of High-Power LEDs With Ceramic Packages
Jianzheng Hu, J, IEEE transactions on device and materials reliability,
ISSN: 1530-4388, Date: 06/2008, Volume: 8, Issue: 2, DOI:
10.1109/TDMR.2008.920298
- Double-Sided Liquid Cooling for Power Semiconductor Devices Using Embedded Power Packaging
Charboneau, B.C, IEEE transactions on industry applications, ISSN:
0093-9994, Date: 09/2008.
- PowerPad™ Thermally Enhanced Package, Steven Kummerl, Texas Instruments, SLMA002G – November 1997 – Revised January 2011

- Materials for the 2020 Challenges: The View of Industry , Carmelo Papa, Executive Vice president, Industrial and Multisegment General Manager, STMicroelectronics
- High Voltage Half Bridge Design Guide for LMG3410 Smart GaN FET, Texas Instruments, SNOA946-April 2016, Eric Faraci and Jie Mao.
- Development and Characterization of the Thermal behaviour of packaged Cascode GaN HEMT's, Chou, Hsin-Ping, ISSN:1369:8001, Date:01/2016, Vol:41
- M. Garven and J. P. Calame, "Simulation and optimization of gate temperatures in GaN-on-SiC monolithic microwave integrated circuits," *IEEE Trans. Components and Packaging Technol.*, vol. 32, no. 1, Mar. 2009, pp. 63-72.
- Characterization and thermal analysis of packaged AlGaIn/GaN power HEMT
Date of Conference: 19-21 Oct. 2011, **INSPEC Accession Number:** 12461619, **Date Added to IEEE Xplore:** 29 December 2011, **DOI:** [10.1109/IMPACT.2011.6117287](https://doi.org/10.1109/IMPACT.2011.6117287), Electronic ISBN: 978-1-4577-1389-7,

Print ISBN: 978-1-4577-1387-3, Online ISBN: 978-1-4577-1388-0, Print on Demand(PoD) ISBN: 978-1-4577-1387-3, USB ISBN: 978-1-4577-1388-0 (Curing of TIM Material therefore mismatch between experimental and simulation data)

- GaN-Based RF Power Devices and Amplifiers
Mishra UK, Proceedings of IEEE, ISSN: 0018-9219, Date: 02/2008,

- An Introduction to GaN-on-Si Power Device Technology, Huga Optotech.Inc

- Images for models referred from
 1. <https://cdn.macom.com/datasheets/MAGX-011086.pdf>
 2. <http://www.wolfspeed.com/downloads/dl/file/id/314/product/116/cgh40006s.pdf>

- Solid and surface material properties:
 1. <https://www.omega.com/literature/transactions/volume1/emissivitya.htm>
↓
 2. <https://ntrs.nasa.gov/archive/nasa/casi.ntrs.nasa.gov/19690022517.pdf>

3. <http://www.almit.com/dloads/Agents/SAC%20Alloy%20Comparison.pdf>
4. https://www.google.com/#q=Density+of+SAC305&*
5. https://www.google.com/#q=Density+of+GaN&*
6. <http://www.ioffe.ru/SVA/NSM/Semicond/GaN/thermal.html>
7. [http://www.ametek-ecp.com/-/media/ametek
ecp/files/cwtechnicalpapers/coining_english_gold_tin_paper.pdf](http://www.ametek-ecp.com/-/media/ametek
ecp/files/cwtechnicalpapers/coining_english_gold_tin_paper.pdf)
8. [http://www.matweb.com/search/datasheet.aspx?matguid=c3e81a488d6
e4e829014b0b214ed4255&ckck=1](http://www.matweb.com/search/datasheet.aspx?matguid=c3e81a488d6
e4e829014b0b214ed4255&ckck=1)

Biographical Information

Tanmay Kavade completed his undergraduate degree in Mechanical Engineering from the University of Pune, India in May 2011. He also completed a post graduate course in steam engineering from Forbes-Marshall Pvt. Ltd. He worked as an Engineer – Sales at GreenTechnology and Contracting L.L.C in Doha, Qatar from November 2012 – May 2014. He started his work in package level thermal analysis of GaN HEMT under Dr Dereje Agonafer's guidance for Master's Degree in August 2016.

His research interest includes package level thermal analysis, data center cooling, computational fluid dynamics, thermal and fluid sciences.